

# Nanoformulation of D- $\alpha$ -tocopheryl polyethylene glycol 1000 succinate-b-poly( $\epsilon$ -caprolactone-ran-glycolide) diblock copolymer for siRNA targeting HIF-1 $\alpha$ for nasopharyngeal carcinoma therapy

Yuhan Chen<sup>1,\*</sup>Gang Xu<sup>1,\*</sup>Yi Zheng<sup>2-4</sup>Maosheng Yan<sup>1</sup>Zihuang Li<sup>1</sup>Yayan Zhou<sup>1</sup>Lin Mei<sup>2-4</sup>Xianming Li<sup>1</sup>

<sup>1</sup>Department of Radiation Oncology, Second Clinical Medicine College of Jinan University, Shenzhen, Guangdong, People's Republic of China; <sup>2</sup>The Shenzhen Key Laboratory of Gene and Antibody Therapy, Center for Biotechnology and BioMedicine, <sup>3</sup>Division of Life Sciences and Health, Graduate School at Shenzhen, Tsinghua University, Shenzhen, Guangdong Province, People's Republic of China; <sup>4</sup>School of Life Sciences, Tsinghua University, Beijing, People's Republic of China

\*These authors contributed equally to this work

**Abstract:** Hypoxia-inducible factor-1 $\alpha$  (HIF-1 $\alpha$ ) is a crucial transcription factor that plays an important role in the carcinogenesis and development of nasopharyngeal carcinoma. In this research, a novel biodegradable D- $\alpha$ -tocopheryl polyethylene glycol 1000 succinate-b-poly( $\epsilon$ -caprolactone-ran-glycolide) (TPGS-b-(PCL-ran-PGA)) nanoparticle (NP) was prepared as a delivery system for small interfering ribonucleic acid (siRNA) molecules targeting HIF-1 $\alpha$  in nasopharyngeal carcinoma gene therapy. The results showed that the NPs could efficiently deliver siRNA into CNE-2 cells. CNE-2 cells treated with the HIF-1 $\alpha$  siRNA-loaded TPGS-b-(PCL-ran-PGA) NPs showed reduction of HIF-1 $\alpha$  expression after 48 hours of incubation via real-time reverse transcriptase-polymerase chain reaction and Western blot analysis. The cytotoxic effect on CNE-2 cells was significantly increased by HIF-1 $\alpha$  siRNA-loaded NPs when compared with control groups. In a mouse tumor xenograft model, the HIF-1 $\alpha$  siRNA-loaded NPs efficiently suppressed tumor growth, and the levels of HIF-1 $\alpha$  mRNA and protein were significantly decreased. These results suggest that TPGS-b-(PCL-ran-PGA) NPs could function as a promising genetic material carrier in antitumor therapy, including therapy for nasopharyngeal carcinoma.

**Keywords:** TPGS-b-(PCL-ran-PGA), nanoparticles, nasopharyngeal carcinoma, hypoxia-inducible factor-1 $\alpha$ , gene delivery

## Introduction

Nasopharyngeal carcinoma (NPC) is one of the most common head and neck cancers in the People's Republic of China and in Southeast Asia.<sup>1</sup> The definitive treatment for early-stage NPC is radiotherapy, while for the advanced stage, treatment involves radiotherapy plus cisplatin-based chemotherapy. Although NPC is sensitive to radiotherapy, with regard to all stages of NPC, the 5-year overall survival rate ranges from 32% to 62% worldwide.<sup>2</sup> The poor survival of NPC patients can be ascribed to local recurrence and distant metastasis. Thus, there is an urgent need both to better understand the mechanism of NPC development and to develop novel therapeutic strategies for NPC.

Hypoxia has been viewed as a common biological characteristic of many malignancies. Tumor hypoxia is known to contribute to tumor phenotype by influencing angiogenesis, invasiveness, and metastasis, in addition to leading to resistance of tumor to radiotherapy and chemotherapy.<sup>3</sup> Previous studies have shown that a key transcription factor termed hypoxia-inducible factor (HIF-1) is involved in regulating the adaptive response to hypoxia conditions.<sup>4</sup> HIF-1 is a heterodimer consisting of two subunits:

Correspondence: Xianming Li  
Department of Radiation Oncology,  
Second Clinical Medicine College of Jinan  
University, 1017 Dongmen North Road,  
Shenzhen, Guangdong 518020, People's  
Republic of China  
Tel +86 755 2553 3018  
Email lxm1828@hotmail.com

HIF-1 $\alpha$  and HIF-1 $\beta$ . In particular, the HIF-1 pathway is mainly mediated through the stability and activity of HIF-1 $\alpha$ .<sup>5</sup> HIF-1 $\alpha$  induces the expression of several downstream genes, influencing many aspects of tumor biology, such as cellular energy metabolism, growth rate, angiogenesis, invasiveness, metastasis, and apoptosis.<sup>6</sup> Several studies have found that HIF-1 $\alpha$  overexpression is associated with the poor prognosis in NPC,<sup>7–9</sup> which has generated widespread interest in the use of HIF-1 $\alpha$  therapeutics as novel treatment candidates.

Through a mechanism known as RNA interference (RNAi), small interfering RNA (siRNA) molecules can bring together complementary mRNA strands of target genes for degradation, thus specifically downregulating gene expression.<sup>10</sup> Recently, many researchers have paid greater attention to the application of nonviral vectors, with advantages of easy preparation, good biocompatibility, nonpathogenicity, and nonimmunogenicity, in the delivery of siRNA into target cells.<sup>11–14</sup> Various types of nonviral vectors, such as dendrimers,<sup>15</sup> liposomes,<sup>16</sup> polycationic polymers,<sup>17,18</sup> and polymeric nanoparticles (NPs),<sup>19</sup> have been investigated for application in gene delivery. Among these carrier systems, NPs could serve as ideal vectors for siRNA delivery because of their small diameter, sustained-release features, and ability to increase transfection efficiency with low cytotoxicity.<sup>20–22</sup>

In the present research, a novel biodegradable copolymer, D- $\alpha$ -tocopheryl polyethylene glycol 1000 succinate-b-poly( $\epsilon$ -caprolactone-ran-glycolide) (TPGS-b-[PCL-ran-PGA]), has been successfully synthesized as the carrier for delivery of gene-targeting therapy.<sup>23</sup> Favorable characteristics such as longer half-life, higher encapsulation efficiency, increased cellular uptake, and greater therapeutic efficiency of the formulated drug have been observed for TPGS-emulsified NPs than those emulsified by polyvinyl alcohol (PVA).<sup>24</sup> As a water-soluble derivative of naturally sourced vitamin E, TPGS is capable of improving drug permeability by inhibiting the P-glycoprotein (P-gp) pumps and thus increasing the absorption of drug and reducing the P-gp pump-mediated multidrug resistance of tumor cells.<sup>25,26</sup> Moreover, TPGS inhibits tumor growth in cell lines and animal models by inducing cancer cell apoptosis, which has been applied in the exploration of synergistic anticancer effects through combinations of TPGS with other anticancer agents.<sup>27–29</sup> Copolymerization of PCL with PGA could improve polymer biocompatibility and biodegradability, as well as controlling drug release. Our previous studies have confirmed that TPGS-b-(PCL-ran-PGA) NPs can successfully deliver antitumor drugs and plasmid DNA

into cancer cells and effectively inhibit tumor growth.<sup>23,30,31</sup> Considering these results, we hypothesized that TPGS-b-(PCL-ran-PGA) NPs could deliver HIF-1 $\alpha$  siRNA into NPC cell CNE-2 and thus facilitate exploitation of the antitumor effects of siRNA. Thus, we prepared siRNAs targeting HIF-1 $\alpha$ -loaded TPGS-b-(PCL-ran-PGA) NPs for anti-NPC therapy and investigated the antitumor effects of such NPs in vitro and in vivo.

## Materials and methods

### Materials

TPGS-b-(PCL-ran-PGA) copolymer (molecular weight: approximately 24,000 Da) was synthesized in our laboratory at the School of Life Sciences, Tsinghua University, People's Republic of China.<sup>23</sup> TPGS, glycolide (1,4-dioxane-2,5-dione), PVA (80% hydrolyzed), and 3-(4,5-dimethylthiazol-2-yl)-2,5-diphenyl-2H-tetrazolium bromide (MTT) were purchased from Sigma-Aldrich (St Louis, MO, USA).  $\epsilon$ -Caprolactone was obtained from Acros Organics (Geel, Belgium). 4',6-Diamidino-2-phenylindole dihydrochloride (DAPI) was obtained from Vector Laboratories (Burlingame, CA, USA). RPMI medium 1640 (basic), fetal bovine serum, penicillin–streptomycin, and phosphate-buffered saline (PBS) were acquired from Invitrogen–Gibco (Carlsbad, CA, USA). All other chemicals and solvents used were of the highest quality commercially available.

### SiRNA

HIF-1 $\alpha$ -targeting siRNA and fluorescent Carboxyfluorescein (FAM)-labeled siRNA (FAM–siRNA) were purchased from GenePharma Co, Ltd (Suzhou, Jiangsu, People's Republic of China). The siRNAs had the following sequences – sense: 5'–GGAAUGAGAGAAAUGCUUTT–3'; antisense: 5'–AAGCAUUUCUCUCAUUUCCTT–3'. The scrambled control for HIF-1 $\alpha$  siRNA was also purchased from GenePharma Co, Ltd (Suzhou). RNase-free diethyl pyrocarbonate (DEPC)-treated Milli-Q water was used for all dilutions.

### Preparation of the siRNA-loaded TPGS-b-(PCL-ran-PGA) NPs

The siRNA-loaded TPGS-b-(PCL-ran-PGA) NPs were prepared using a double-emulsion method. In brief, 50  $\mu$ L of 20  $\mu$ M siRNA solution in DEPC-treated Milli-Q water was emulsified with 250  $\mu$ L of dichloromethane containing 5 mg of TPGS-b-(PCL-ran-PGA) by sonication for 60 seconds to obtain a water-in-oil (w/o) emulsion. PVA (1 mL of a 2% w/v solution) was added to the emulsion, and the mixture was then sonicated 12 times (5-second sonication and 5-second

arrest) to form a water-in-oil-in-water (w1/o/w2) double emulsion. The resulting emulsion was subsequently diluted with 5 mL of 2% (w/v) PVA and stirred for 1.5 hours at room temperature for evaporation of dichloromethane. Finally, the NPs were centrifuged at 18,000 $\times g$  for 15 minutes at 4°C and washed twice with 6 mL of RNase-free water to remove the PVA and untrapped siRNA before further characterization.

### Characterization of NPs

The mean particle size of the NPs was determined using dynamic light scattering (Zetasizer Nano ZS90; Malvern Instruments Ltd, Malvern, UK). Briefly, NPs (1 mg) were suspended in DEPC-treated Milli-Q water at a concentration of 0.5 mg/mL. The zeta-potential of the NPs was measured by laser Doppler anemometry (Zetasizer Nano ZS90). The particles were diluted with deionized water to ensure that the zeta-potential of the NPs can be characterized accurately under conditions of low ionic strength. The final concentration of the polymer was 1 mg/mL. The particle morphology was assessed by transmission electron microscopy. All measurements were performed in triplicate.

### Evaluation of encapsulation efficiency of siRNA in the NPs

The encapsulation efficiency of siRNA-loaded NPs was the percentage of siRNA encapsulated in the NPs to the total amount of siRNA initially added. Briefly, 1 mg of NPs in 250  $\mu$ L chloroform was added into 500  $\mu$ L Tris-ethylenediamine tetraacetic acid buffer and then rotated for 30 minutes at room temperature to extract siRNA from the organic phase into the aqueous phase, followed by centrifugation at 4°C and 18,000 $\times g$  for 20 minutes. The siRNA concentration in the supernatant was then assayed using an ultraviolet (UV) spectrophotometer (Beckman, Fullerton, CA, USA) at 260 nm.

### In vitro release assay

About 1 mg of siRNA-loaded TPGS-b-(PCL-ran-PGA) NPs was suspended in 1 mL of PBS buffer at pH 7.4 or 4.0 in RNase-free Eppendorf tubes and placed on a rotary shaker at 100 rpm at 37°C. At designated time intervals, after the tubes were centrifuged at 12,000 rpm/min for 20 minutes at 4°C, the supernatants were removed and the NP deposits were resuspended with fresh buffer solution. The amount of siRNA in the supernatant was measured at 260 nm with a UV spectrophotometer.

### Cell culture

CNE-2 cells (American Type Culture Collection, Manassas, VA, USA) were cultured in RPMI 1640 (pH 7.4) containing 10  $\mu$ g/mL streptomycin sulfate, 100  $\mu$ g/mL penicillin G, and 10% (v/v) fetal bovine serum. Cells were incubated at 37°C in a 5% CO<sub>2</sub>, 95% air incubator.

### Confocal laser scanning microscopy observation of the siRNA-loaded NPs

The cells were seeded in a six-well ( $3 \times 10^5$  cells per well) plate and cultured for 24 hours at 37°C in 5% CO<sub>2</sub>. In order to obtain confocal laser scanning microscopy (CLSM) observation of the cellular uptake of siRNA, the siRNA was labeled with FAM. FAM-siRNA targeting HIF-1 $\alpha$ , FAM-scrambled siRNA-loaded TPGS-b-(PCL-ran-PGA) NPs, or FAM-siRNA targeting HIF-1 $\alpha$ -loaded TPGS-b-(PCL-ran-PGA) NPs were added separately to the plate, and the mixture was incubated for 4 hours at 37°C. The cells were rinsed three times with PBS and then fixed in 4% paraformaldehyde for 20 minutes at room temperature. The nuclei were stained with DAPI for 5 minutes at room temperature, avoiding light, and washed three times with PBS. Finally, the cellular uptake of the siRNA-loaded NPs was observed using a confocal laser scanning microscope (Fluoview FV-1000, Olympus Optical Co, Ltd, Tokyo, Japan).

### Effect of siRNA-loaded TPGS-b-(PCL-ran-PGA) NPs on HIF-1 $\alpha$ expression in CNE-2 cells

Real-time polymerase chain reaction (PCR) and Western blot assay were used to determine the HIF-1 $\alpha$  mRNA and protein levels, respectively, after RNAi. The CNE-2 cells were cultured in a six-well plate overnight to facilitate attachment to the substrate. Before conducting RNA interference, the cells were incubated with CoCl<sub>2</sub> (100  $\mu$ M), a chemical hypoxia-inducible reagent, to simulate the tumor hypoxia microenvironment. CNE-2 cells without any treatment served as the normal control. The naked siRNA targeting HIF-1 $\alpha$ , blank TPGS-b-(PCL-ran-PGA) NPs, scrambled siRNA-loaded TPGS-b-(PCL-ran-PGA) NPs, or siRNA targeting HIF-1 $\alpha$ -loaded TPGS-b-(PCL-ran-PGA) NPs was added separately into each well. The final concentration of siRNA in these NPs was 50 nM.

### Real-time PCR

Total RNA from the samples was extracted using TRIzol reagent (Invitrogen). Reverse transcription was conducted using the Prime Script RT reagent Kit (Takara

Bio, Japan). Subsequent PCR amplification was carried out with primer sequences to HIF-1 $\alpha$  (sense primer: 5'-CAAACACACAGCGAAGC-3'; antisense primer: 5'-TCAACCCAGACATATCCACC-3') and to glyceraldehyde 3-phosphate dehydrogenase (GAPDH) (sense primer: 5'-ATGGTGGTGAAGACGCCAGTA-3'; antisense primer: 5'-GGCACAGTCAAGGGCTGAGAATG-3'). Quantitative PCR amplification was performed in a real-time fluorescent measurement system (ABI7300, USA) using the iTaq™ Universal SYBR® Green Supermix (Bio-Rad, USA) according to the manufacturer's instructions. The HIF-1 $\alpha$  mRNA levels were normalized using GAPDH.

### Western blot

After 48 hours of incubation at 37°C, the cells were lysed in cell lysis buffer containing phenylmethylsulfonyl fluoride for 30 minutes at 4°C. Then the cell lysate was centrifuged at 13,000 rpm for 20 minutes at 4°C. The proteins were then separated via sodium dodecyl sulfate polyacrylamide gel electrophoresis and electrotransferred to the polyvinylidene fluoride membrane (Immobion-P Transfer Membrane; Millipore Corp, Billerica, MA, USA). Tris-buffered saline with 0.1% Tween-20 solution containing 5% nonfat dry milk was used to block the membranes and after that, the membranes were exposed to anti-human HIF-1 $\alpha$  antibody for further incubation overnight at 4°C. The immunoreactive signals were detected by chemiluminescence using an enhanced chemiluminescence detection kit. Anti-GAPDH antibody was used as loading control.

### Cell viability

The cytotoxicity of the TPGS-b-(PCL-ran-PGA) NPs was determined using the MTT assay in CNE-2 cells. Briefly, the cells were cultured in 96-well plates at a density of 10,000 cells per well and incubated for 24 hours. Blank TPGS-b-(PCL-ran-PGA), naked siRNA targeting HIF-1 $\alpha$ , scrambled siRNA-loaded TPGS-b-(PCL-ran-PGA) NPs, or siRNA targeting HIF-1 $\alpha$ -loaded TPGS-b-(PCL-ran-PGA) NPs was added into each well at different concentrations. There were three wells for each mixture. Twenty-four hours after transfection, 20  $\mu$ L of MTT solution (5 mg/mL) was added to each well. After 4 hours of incubation at 37°C under a humidified atmosphere supplemented with 5% CO<sub>2</sub> in air, the culture medium was removed and then 100  $\mu$ L of dimethyl sulfoxide was added to each well to dissolve the MTT formazan crystals. The cell viability was evaluated by measuring the absorbance of formazan products at 490 nm using a microplate reader.

### In vivo experiment

Female BALB/c-nu/nu mice were obtained from the Medical Experimental Animal Center of Guangdong Province (Guangdong, People's Republic of China). All the animals were kept in filter-topped cages under standard conditions with food and water ad libitum. The studies were performed in conformity with the recommendations in the Guide for the Care and Use of Laboratory Animals of Institutional Animal Care and Use Committee of Graduate School at Shenzhen, Tsinghua University. The experimental procedures were ethically approved by the Animal Welfare and Ethics Committee of Graduate School at Shenzhen, Tsinghua University, People's Republic of China (number 2011-YZ-BG). First, subcutaneous tumors were developed by inoculation of 2 $\times$ 10<sup>6</sup> CNE-2 cells in the flank region of 6-week-old female nude mice (18 $\pm$ 2 g). When the tumor grew to approximately 5–7 mm in diameter, the mice were randomly divided into the following groups (n=5): blank TPGS-b-(PCL-ran-PGA), naked siRNA targeting HIF-1 $\alpha$ , scrambled siRNA-loaded TPGS-b-(PCL-ran-PGA) NPs, and siRNA targeting HIF-1 $\alpha$ -loaded TPGS-b-(PCL-ran-PGA) NPs. The groups were treated with a dose of 0.3 mg siRNA/kg body weight by intratumoral injections every 3 days for a total of five times. The tumor diameters were measured using a electronic caliper, and tumor volume was calculated as follows: longest diameter  $\times$  shortest diameter<sup>2</sup>/2. On the second day after the final treatment, mice were sacrificed to measure the tumor weight, and tumor tissues were collected to evaluate the expression of HIF-1 $\alpha$  mRNA and protein by real-time PCR and Western blotting, respectively. In addition, tumor samples were fixed with 10% neutral formalin to prepare paraffin-embedded sections for hematoxylin and eosin (H&E) staining.

### Statistical analyses

Quantitative data were expressed as the mean  $\pm$  standard deviation. Student's *t*-test for two groups and one-way analysis of variance for multiple groups were performed with SPSS 16.0 software (Chicago, IL, USA). *P*<0.05 was considered to be statistically significant.

## Results

### Characterization of NPs

Our laboratory has successfully synthesized a novel biodegradable copolymer termed TPGS-b-(PCL-ran-PGA), which has been well investigated as a carrier system to deliver drugs and genes into cells. By dynamic light scattering, blank TPGS-b-(PCL-ran-PGA) NPs and siRNA-loaded TPGS-b-(PCL-ran-PGA) NPs were found to have an average diameter



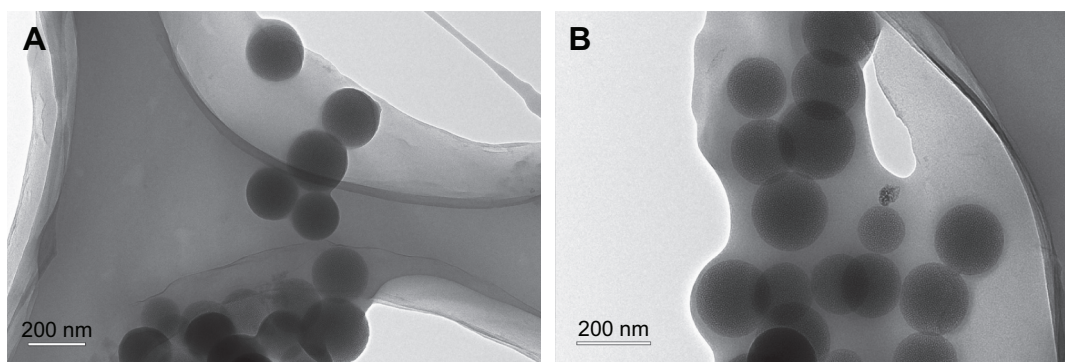


**Figure 1** TEM images of blank TPGS-b-(PCL-ran-PGA) nanoparticles (A) and siRNA-loaded TPGS-b-(PCL-ran-PGA) nanoparticles (B).

**Abbreviations:** TEM, transmission electron microscopy; TPGS-b-(PCL-ran-PGA), D- $\alpha$ -tocopheryl polyethylene glycol 1000 succinate-b-poly( $\epsilon$ -caprolactone-ran-glycolide); siRNA, small interfering ribonucleic acid.

of  $246.84 \pm 3.25$  nm and  $275.72 \pm 2.94$  nm, respectively. The zeta-potential of blank TPGS-b-(PCL-ran-PGA) NPs and siRNA-loaded TPGS-b-(PCL-ran-PGA) NPs were found to be approximately  $-19.36 \pm 2.47$  mV and  $-23.18 \pm 1.70$  mV, respectively. As Figure 1 shows, both blank TPGS-b-(PCL-ran-PGA) NPs and siRNA-loaded TPGS-b-(PCL-ran-PGA) NPs were spherical in shape. The encapsulation efficiency of siRNA-loaded TPGS-b-(PCL-ran-PGA) NPs was  $70.20\% \pm 1.91\%$ .

### In vitro release

The in vitro release profile of siRNA-loaded TPGS-b-(PCL-ran-PGA) NPs was investigated at pH 4.0 and pH 7.4. siRNA release was determined by measuring UV absorption at 260 nm for each time interval, namely, 1, 2, 4, 6, 12, 24, 48, 72, and 96 hours. As shown in Figure 2, the cumulative release rates of siRNA over a period of 24 hours at pH 4.0 and pH 7.4 were  $56.27\% \pm 3.15\%$  and  $42.85\% \pm 3.63\%$ , respectively. At 96 hours postincubation, the amounts of cumulative siRNA released from TPGS-b-(PCL-ran-PGA) NPs at

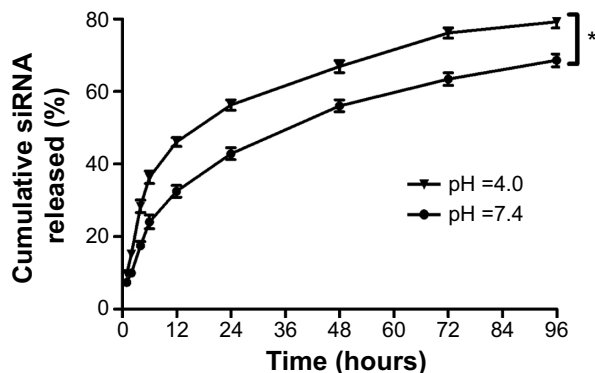


**Figure 2** In vitro release profile of siRNA from nanoparticles that were diluted in PBS at different pHs.

**Notes:** Data are given as the means  $\pm$  SD ( $n=5$ ). \*Significant ( $P<0.05$ ) increase of siRNA release at pH=4.0 compared with that at pH=7.4.

**Abbreviations:** siRNA, small interfering ribonucleic acid; SD, standard deviation.

pH 4.0 and pH 7.4 were  $79.22\% \pm 3.86\%$  and  $68.61\% \pm 3.95\%$ , respectively. The release kinetics of siRNA from NPs at pH 4.0 was more rapid than that at pH 7.4 ( $P<0.05$ ).

### CLSM observation of the siRNA-loaded NPs

CLSM was used to evaluate the TPGS-b-(PCL-ran-PGA) NP-mediated delivery of siRNA into the cells. Figure 3 shows the results after the CNE-2 cells were incubated with FAM-siRNA targeting HIF-1 $\alpha$ , FAM-scrambled siRNA-loaded TPGS-b-(PCL-ran-PGA) NPs, or FAM-siRNA targeting HIF-1 $\alpha$ -loaded TPGS-b-(PCL-ran-PGA) NPs for 4 hours. No obvious fluorescence of FAM-siRNA was observed in cells that were transfected with naked FAM-siRNA. However, the fluorescence intensity of FAM-siRNA was significantly strong in cells treated with FAM-scrambled siRNA or FAM-siRNA targeting HIF-1 $\alpha$ -loaded TPGS-b-(PCL-ran-PGA) NPs. As depicted in Figure 3F and I, the fluorescence of FAM-siRNA (green) was closely located around the nuclei (blue, stained by DAPI).

### Effect of siRNA-loaded TPGS-b-(PCL-ran-PGA) NPs on HIF-1 $\alpha$ expression in CNE-2 cells

In the in vitro transfection experiments, the levels of HIF-1 $\alpha$  mRNA and protein were determined by real-time PCR and Western blotting, respectively. CNE-2 cells without any treatment served as the normal control. Cells treated with scrambled siRNA-loaded TPGS-b-(PCL-ran-PGA) NPs were used as the negative control. The real-time PCR results showed that the HIF-1 $\alpha$  mRNA level of CNE-2 exhibited an approximately 62% decrease following transfection with siRNA targeting HIF-1 $\alpha$ -loaded TPGS-b-(PCL-ran-PGA) NPs, compared with the normal control (Figure 4A). The Western blot results confirmed the real-time PCR results.

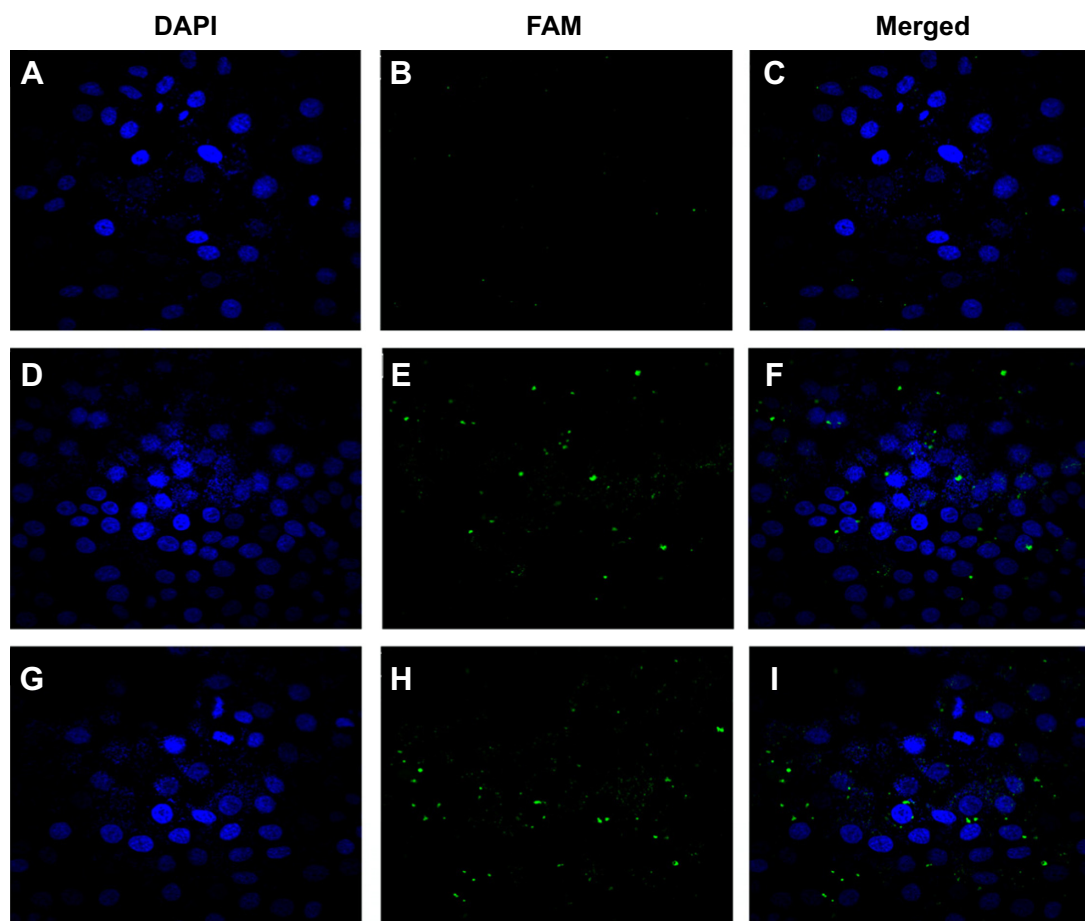


**Figure 3** Confocal laser scanning microscopy images of CNE-2 cells' uptake of NP-mediated siRNA transfection.

**Notes:** (A–C) Cells were incubated with FAM-siRNA. (D–F) Cells were incubated with FAM-scrambled siRNA-loaded TPGS-b-(PCL-ran-PGA) NPs. (G–I) Cells were incubated with FAM-siRNA targeting HIF-1 $\alpha$ -loaded TPGS-b-(PCL-ran-PGA) NPs. Green color: FAM-labeled siRNAs. Blue color: cell nuclei stained by DAPI.

**Abbreviations:** DAPI, 4',6-diamidino-2-phenylindole dihydrochloride; FAM, carboxyfluorescein; HIF-1 $\alpha$ , hypoxia-inducible factor-1 $\alpha$ ; NP, nanoparticle; TPGS-b-(PCL-ran-PGA), D- $\alpha$ -tocopheryl polyethylene glycol 1000 succinate-b-poly( $\epsilon$ -caprolactone-ran-glycolide); siRNA, small interfering ribonucleic acid.

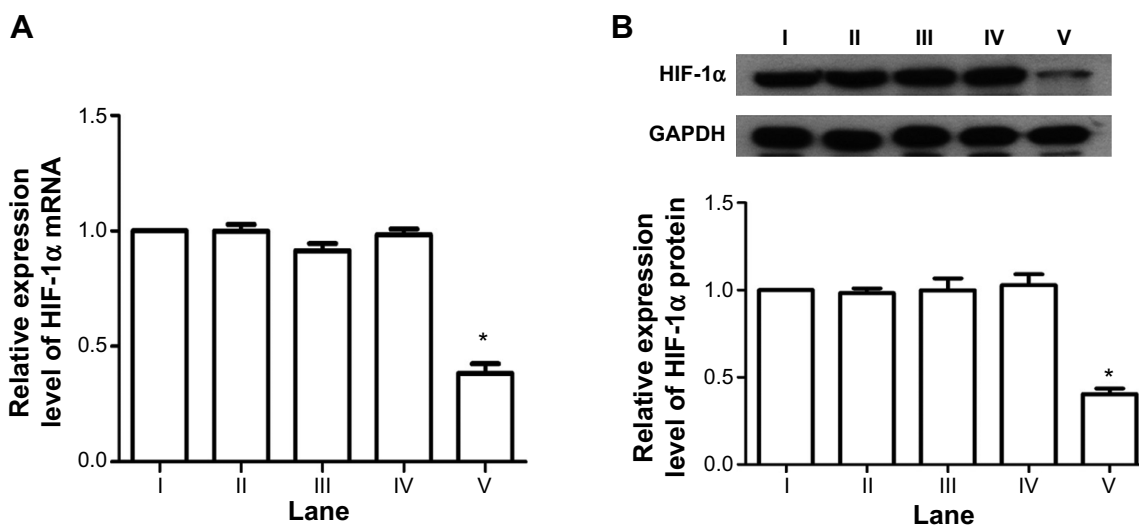


**Figure 4** The expression level of HIF-1 $\alpha$  determined by real-time PCR (A) and Western blotting (B) in the in vitro transfection experiments.

**Notes:** Lane I: cells without treatment; Lane II: cells treated with siRNA targeting HIF-1 $\alpha$ ; Lane III: cells treated with blank TPGS-b-(PCL-ran-PGA) NPs; Lane IV: cells treated with scrambled siRNA-loaded TPGS-b-(PCL-ran-PGA) NPs; Lane V: cells treated with siRNA targeting HIF-1 $\alpha$ -loaded TPGS-b-(PCL-ran-PGA) NPs. The HIF-1 $\alpha$  mRNA and protein levels were normalized using GAPDH mRNA and protein levels, respectively. \*Significant ( $P < 0.05$ ) decrease in expression level of HIF-1 $\alpha$  compared with the other four groups.

**Abbreviations:** GAPDH, glyceraldehyde 3-phosphate dehydrogenase; HIF-1 $\alpha$ , hypoxia-inducible factor-1 $\alpha$ ; NP, nanoparticle; TPGS-b-(PCL-ran-PGA), D- $\alpha$ -tocopheryl polyethylene glycol 1000 succinate-b-poly( $\epsilon$ -caprolactone-ran-glycolide); PCR, polymerase chain reaction; siRNA, small interfering ribonucleic acid.

In comparison with the normal control, the expression level of HIF-1 $\alpha$  protein was only 40.4% in the cells treated with siRNA targeting HIF-1 $\alpha$ -loaded TPGS-b-(PCL-ran-PGA) NPs (Figure 4B), whereas the expression levels of HIF-1 $\alpha$  mRNA and protein were not significantly different among the normal control, negative control, naked siRNA, and blank TPGS-b-(PCL-ran-PGA) NP treatment groups.

## Cell viability

Cytotoxicity of NPs was determined at different concentrations using the MTT assay. Cells treated with NP concentration of 0  $\mu\text{g/mL}$  were considered to be the control. As shown in Figure 5, with increasing dosage of TPGS-b-(PCL-ran-PGA) NPs, a slight decrease of cell viability was observed; similar results were observed in cells treated with scrambled siRNA-loaded TPGS-b-(PCL-ran-PGA) NPs. Naked siRNA had no significant cytotoxicity at various dosages. In comparison with the control, TPGS-b-(PCL-ran-PGA) NP-mediated siRNA transfection showed significant effects on cell viability at doses  $>50 \mu\text{g/mL}$  ( $P<0.05$ ).

## In vivo animal experiment

The antitumor effect of siRNA-loaded NPs on tumor regression was evaluated on BALB/c-nu/nu mice. CNE-2 cells were inoculated into nude mice to establish the subcutaneous tumor models, and the tumor volumes were calculated at regular intervals during tumor growth. As shown in Figure 6, there existed significant increases in tumor volumes in the groups treated with naked siRNA, blank TPGS-b-(PCL-ran-PGA) NPs, and scrambled siRNA-loaded TPGS-b-(PCL-ran-PGA) NPs. However, the group treated with siRNA targeting HIF-1 $\alpha$ -loaded TPGS-b-(PCL-ran-PGA) NPs showed significantly

slowed-down tumor growth in comparison with the other three groups ( $P<0.05$ ). Compared with the naked siRNA, blank TPGS-b-(PCL-ran-PGA) NPs and scrambled siRNA-loaded TPGS-b-(PCL-ran-PGA) NPs could also have slight anticancer efficacy ( $P<0.05$ ). Tumor weights were measured after the mice were sacrificed, and the data showed that the tumor weights in the group treated with siRNA targeting HIF-1 $\alpha$ -loaded TPGS-b-(PCL-ran-PGA) NPs were much lower than those of the other three groups ( $P<0.05$ ) (Figure 7). The differences in the inhibitory effect on tumor sizes among the different treatment groups can be observed in Figure 8. The expression levels of HIF-1 $\alpha$  mRNA and protein in the tumor tissues were significantly decreased after treatment with siRNA targeting HIF-1 $\alpha$ -loaded TPGS-b-(PCL-ran-PGA) NPs (Figure 9). The images of H&E staining also indicated that tumor cell necrosis and apoptosis were markedly increased in the group treated with siRNA targeting HIF-1 $\alpha$ -loaded TPGS-b-(PCL-ran-PGA) NPs, in comparison with the same in the other three groups (Figure 10).

## Discussion

As a transcription factor, HIF-1 $\alpha$  is activated to mediate the adaptive response to intratumoral hypoxia in human cancer. Under hypoxic conditions, HIF-1 $\alpha$  upregulates the expression of various genes participating in cell physiological activities, including cell glycolysis, proliferation, angiogenesis, and apoptosis.<sup>6</sup> HIF-1 $\alpha$  plays an important role in tumor growth and in vivo studies have clearly confirmed that there was a significant decrease in the tumor volume through inhibition of HIF-1 $\alpha$  activity.<sup>32-34</sup> HIF-1 $\alpha$  thus becomes the target gene and several selective therapeutic agents including siRNA have been used to suppress cancer growth.<sup>35</sup> siRNA can activate

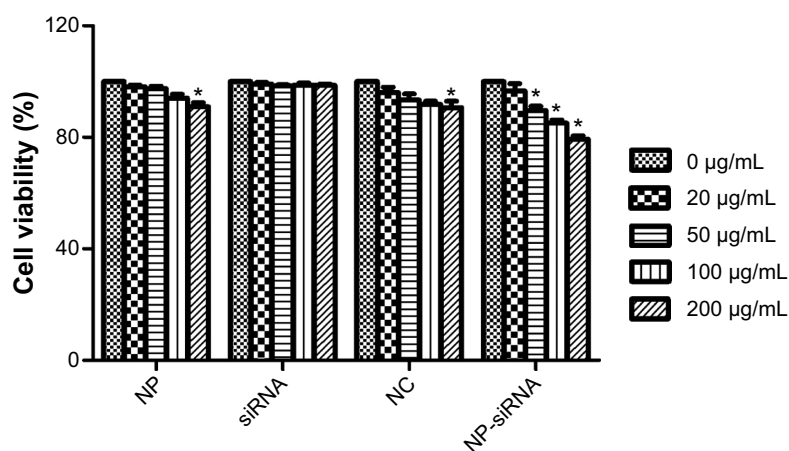


**Figure 5** In vitro cytotoxicity of different concentrations of nanoparticles after incubation of CNE-2 cells for 48 hours.

**Notes:** Data are given as the means  $\pm$  SD ( $n=3$ ). \*Significant ( $P<0.05$ ) increase of cytotoxicity on CNE-2 cells compared with the control group.

**Abbreviations:** HIF-1 $\alpha$ , hypoxia-inducible factor-1 $\alpha$ ; NP, blank TPGS-b-(PCL-ran-PGA) nanoparticles; NC, scrambled siRNA-loaded TPGS-b-(PCL-ran-PGA) nanoparticles; NP-siRNA, siRNA targeting HIF-1 $\alpha$ -loaded TPGS-b-(PCL-ran-PGA) nanoparticles; SD, standard deviation; siRNA, small interfering ribonucleic acid; TPGS-b-(PCL-ran-PGA), D- $\alpha$ -tocopheryl polyethylene glycol 1000 succinate-b-poly( $\epsilon$ -caprolactone-ran-glycolide).

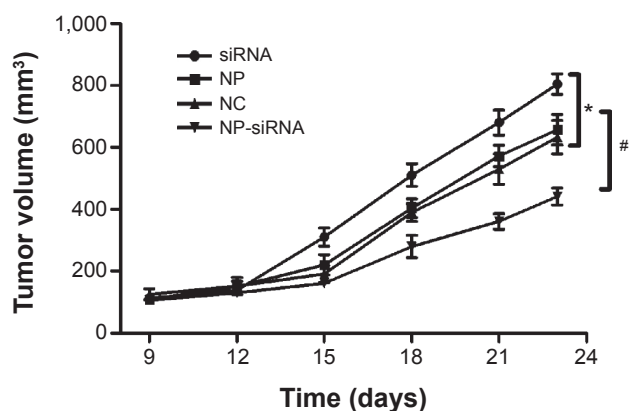


**Figure 6** Antitumor effect of siRNA-loaded TPGS-b-(PCL-ran-PGA) nanoparticles on tumor-bearing mice.

**Notes:** Data are given as the means  $\pm$  SD. (n=5). \*Significant ( $P < 0.05$ ) decrease of tumor volume in groups treated with blank TPGS-b-(PCL-ran-PGA) nanoparticles and scrambled siRNA-loaded TPGS-b-(PCL-ran-PGA) nanoparticles compared with the siRNA-treated group. #Significant ( $P < 0.05$ ) decrease of tumor volume in group treated with siRNA targeting HIF-1 $\alpha$ -loaded TPGS-b-(PCL-ran-PGA) nanoparticles compared with the other three groups.

**Abbreviations:** HIF-1 $\alpha$ , hypoxia-inducible factor-1 $\alpha$ ; NP, blank TPGS-b-(PCL-ran-PGA) nanoparticles; NC, scrambled siRNA-loaded TPGS-b-(PCL-ran-PGA) nanoparticles; NP-siRNA, siRNA targeting HIF-1 $\alpha$ -loaded TPGS-b-(PCL-ran-PGA) nanoparticles; SD, standard deviation; siRNA, small interfering ribonucleic acid; TPGS-b-(PCL-ran-PGA), D- $\alpha$ -tocopheryl polyethylene glycol 1000 succinate-b-poly( $\epsilon$ -caprolactone-ran-glycolide).

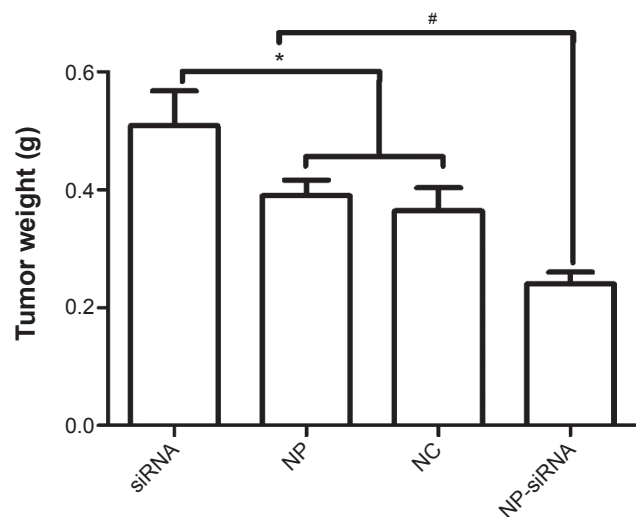


**Figure 7** Comparison of tumor weights of tumor-bearing mice on the second day after the final treatment.

**Notes:** Data are given as the means  $\pm$  SD (n=5). \*Significant ( $P < 0.05$ ) decrease of tumor weights in groups treated with blank TPGS-b-(PCL-ran-PGA) nanoparticles and scrambled siRNA-loaded TPGS-b-(PCL-ran-PGA) nanoparticles compared with the siRNA-treated group. #Significant ( $P < 0.05$ ) decrease of tumor weights in the group treated with siRNA targeting HIF-1 $\alpha$ -loaded TPGS-b-(PCL-ran-PGA) nanoparticles compared with the other three groups.

**Abbreviations:** HIF-1 $\alpha$ , hypoxia-inducible factor-1 $\alpha$ ; NP, blank TPGS-b-(PCL-ran-PGA) nanoparticles; NC, scrambled siRNA-loaded TPGS-b-(PCL-ran-PGA) nanoparticles; NP-siRNA, siRNA targeting HIF-1 $\alpha$ -loaded TPGS-b-(PCL-ran-PGA) nanoparticles; SD, standard deviation; siRNA, small interfering ribonucleic acid; TPGS-b-(PCL-ran-PGA), D- $\alpha$ -tocopheryl polyethylene glycol 1000 succinate-b-poly( $\epsilon$ -caprolactone-ran-glycolide).

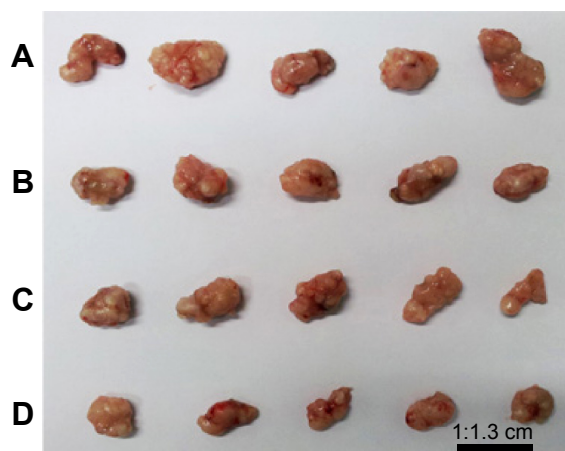


**Figure 8** Macromorphology images of tumor tissues of tumor-bearing mice.

**Notes:** Tumor-bearing mice were treated with naked siRNA (A), blank TPGS-b-(PCL-ran-PGA) NPs (B), scrambled siRNA-loaded TPGS-b-(PCL-ran-PGA) NPs (C), and siRNA targeting HIF-1 $\alpha$ -loaded TPGS-b-(PCL-ran-PGA) NPs (D).

**Abbreviations:** HIF-1 $\alpha$ , hypoxia-inducible factor-1 $\alpha$ ; NP, nanoparticles; siRNA, small interfering ribonucleic acid; TPGS-b-(PCL-ran-PGA), D- $\alpha$ -tocopheryl polyethylene glycol 1000 succinate-b-poly( $\epsilon$ -caprolactone-ran-glycolide).

the endogenous RNAi pathway to mediate sequence-specific gene silencing. However, with respect to the use of siRNA, one of the challenges is to develop an ideal carrier for delivery of siRNA to overcome its limited features of poor stability and insufficient cellular uptake.

In our previous studies, TPGS-b-(PCL-ran-PGA) NPs could be effectively used as an optimizing carrier for delivery of chemotherapeutic drugs and pDNA.<sup>23,30,31</sup> This prompted us to explore whether TPGS-b-(PCL-ran-PGA) NPs could be applied as a vector for siRNA targeting HIF-1 $\alpha$  in NPC gene therapy. The present study showed that these NPs could efficiently deliver siRNA into CNE-2 cells and the expression of HIF-1 $\alpha$  protein decreased significantly, compared with the cells without any treatment. The cytotoxicity on CNE-2 cells was significantly increased by siRNA targeting HIF-1 $\alpha$ -loaded NPs when compared with the control groups. The growth of tumor in nude mouse models was significantly inhibited by siRNA targeting HIF-1 $\alpha$ -loaded TPGS-b-(PCL-ran-PGA) NPs.

In the present work, the encapsulation of siRNA into a polymeric matrix was achieved by the double-emulsion solvent evaporation method, which has been widely developed for the encapsulation of oligonucleotides into a copolymer.<sup>36</sup> In comparison with the preparation process by complexation of siRNA with preformed NPs through electrostatic interaction, adding siRNA to the inner water phase of the double emulsion would enable the siRNA to be encapsulated inside the NP matrix, thus improving the load efficiency. In addition, previous studies have confirmed that encapsulation of siRNA may



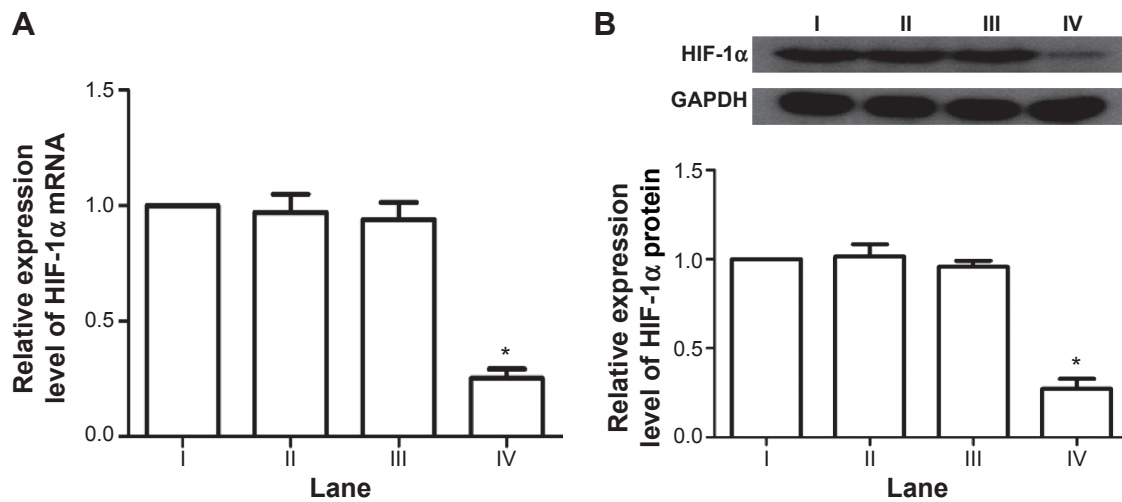


**Figure 9** The expression level of HIF-1 $\alpha$  determined by real-time PCR (A) and Western blotting (B) in tumor tissues.

**Notes:** Lane I: cells treated with naked siRNA; Lane II: cells treated with blank TPGS-b-(PCL-ran-PGA) NPs; Lane III: cells treated with scrambled siRNA-loaded TPGS-b-(PCL-ran-PGA) NPs; Lane IV: cells treated with siRNA targeting HIF-1 $\alpha$ -loaded TPGS-b-(PCL-ran-PGA) NPs. The HIF-1 $\alpha$  mRNA and protein levels were normalized using GAPDH mRNA and protein levels, respectively. \*Significant ( $P < 0.05$ ) decrease in expression level of HIF-1 $\alpha$  compared with the other three groups.

**Abbreviations:** GAPDH, glyceraldehyde 3-phosphate dehydrogenase; HIF-1 $\alpha$ , hypoxia-inducible factor-1 $\alpha$ ; NP, nanoparticle; TPGS-b-(PCL-ran-PGA), D- $\alpha$ -tocopheryl polyethylene glycol 1000 succinate-b-poly( $\epsilon$ -caprolactone-ran-glycolide); PCR, polymerase chain reaction; siRNA, small interfering ribonucleic acid.

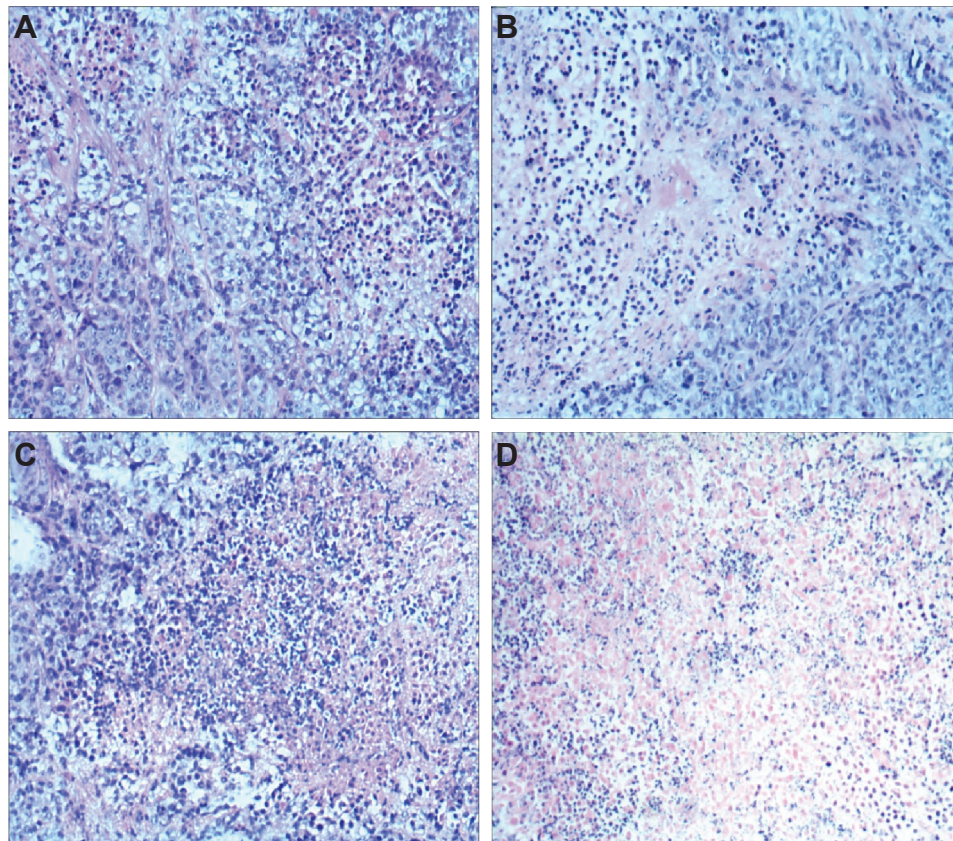


**Figure 10** H&E staining images of tumor tissues of tumor-bearing mice.

**Notes:** Tumor-bearing mice were treated with naked siRNA (A), blank TPGS-b-(PCL-ran-PGA) nanoparticles (B), scrambled siRNA-loaded TPGS-b-(PCL-ran-PGA) nanoparticles (C), and siRNA targeting HIF-1 $\alpha$ -loaded TPGS-b-(PCL-ran-PGA) nanoparticles (D). The scale bar for images (A–D) is magnification  $\times 100$  by microscopy.

**Abbreviations:** HIF-1 $\alpha$ , hypoxia-inducible factor-1 $\alpha$ ; H&E, hematoxylin and eosin; NP, nanoparticle; TPGS-b-(PCL-ran-PGA), D- $\alpha$ -tocopheryl polyethylene glycol 1000 succinate-b-poly( $\epsilon$ -caprolactone-ran-glycolide); siRNA, small interfering ribonucleic acid.

increase the physical protection of siRNA, achieved by some biodegradable NPs, such as poly (lactic-co-glycolic acid), allowing enhanced cellular uptake and sustained release of siRNA against cancer progression-associated genes.<sup>37,38</sup> The results of the present study show that siRNA can be successfully incorporated into biodegradable TPGS-b-(PCL-ran-PGA) NPs with desirable encapsulation efficiency. Particle size and shape are strongly associated with efficiency of gene transfection into the cells and particle distribution within the body. The obtained siRNA-loaded NPs had proper size and were spherical in shape, which is conducive to cellular uptake.

A desirable carrier for delivery would facilitate drug release from treatment formulations at a steady and constant rate over a considerable period. The release pattern of the present study indicated that approximately 50% siRNA is released from TPGS-b-(PCL-ran-PGA) NPs over a period of 24 hours, followed by sustained release during the next 48 hours. The initial burst release phase mainly results from the unencapsulated siRNA on or near the surfaces of NPs and the partial degradation of NPs. The following sustained release phase is primarily due to the slow progressive degradation of NPs, leading to the diffusion of siRNA from the NPs. The TPGS molecule containing polyethylene glycol, which is a hydrophilic molecule, can increase the hydrophilicity of the whole molecule and thus promote the random copolymer to infiltrate and degrade. Copolymerization of PCL with PGA could improve polymer biocompatibility and biodegradability, contributing to control siRNA diffusion through the NP matrix. It was reported that at low pH values, docetaxel (DTX) was released from D- $\alpha$ -tocopheryl polyethylene glycol 1000-block-poly( $\beta$ -amino ester) NPs quickly, while at pH 7.4, the DTX-loaded NPs remained stable.<sup>39</sup> In the present study, the release ratio of siRNA was higher at pH 4.0 than that at pH 7.4, which might be due to the acidification of the microenvironment induced by degradation of the core-shell structure of the NPs.

It is essential to ensure the efficient intracellular transfection and delivery of gene material to exert the advantage of RNAi and exploit the potency of therapeutic activity. The fluorescence of FAM-siRNA-loaded TPGS-b-(PCL-ran-PGA) NPs could be internalized into the cells in the present study. The Figure 3I showed that FAM-siRNA-loaded TPGS-b-(PCL-ran-PGA) NPs were closely located around the nuclei, which further demonstrated that the NPs could efficiently deliver siRNA into CNE-2 cells and this siRNA localization would facilitate gene inhibition or knockdown activity in antitumor therapy.

Determination of gene-silencing activity was performed in CNE-2 cells transfected with naked siRNA targeting HIF-1 $\alpha$ , blank TPGS-b-(PCL-ran-PGA) NPs, scrambled siRNA-loaded TPGS-b-(PCL-ran-PGA) NPs, or siRNA targeting HIF-1 $\alpha$ -loaded TPGS-b-(PCL-ran-PGA) NPs. The expression level of HIF-1 $\alpha$  protein in cells transfected with siRNA-loaded TPGS-b-(PCL-ran-PGA) NPs was decreased significantly compared to that in the naked siRNA- and scrambled siRNA-treated groups, indicating that TPGS-b-(PCL-ran-PGA) NPs could efficiently deliver the siRNA into the cells; the expected silencing effect was strongly correlated with the specificity of the siRNA sequences. Several important molecular regulators involved in cancer progression and apoptosis inhibition, including epidermal growth factor receptor, BH3 interacting domain death agonist, glucose transporter-1, and DNA double-strand break repair enzymes, have been found to be associated with the expression of HIF-1 $\alpha$ ,<sup>40-43</sup> which might explain the relationship between HIF-1 $\alpha$  and cancer cell resistance to apoptosis. Thus, silencing of HIF-1 $\alpha$  may promote tumor cell apoptosis. As the cell viability experiment showed, blank formulations were found to have a slight cytotoxic effect on cell survival with increasing dose, which might be due to the anticancer activity of TPGS that induces apoptosis. Naked siRNA showed nontoxic effects on cell viability, suggesting that siRNA might be degraded before distribution through the cytoplasm. However, siRNA-loaded TPGS-b-(PCL-ran-PGA) NPs appeared to have significant cytotoxicity than the control treatment, the higher cytotoxicity of which may be attributed to the synergistic anticancer activity of the TPGS release from TPGS-b-(PCL-ran-PGA) copolymer and the silencing effect of siRNA targeting HIF-1 $\alpha$  to enhance tumor cell apoptosis.

CNE-2 xenograft tumor models also showed that treatment with TPGS-b-(PCL-ran-PGA) NPs containing HIF-1 $\alpha$  siRNA could effectively inhibit the growth of tumor compared to blank NPs, naked siRNA, and scrambled siRNA-NP-treated group, demonstrating that TPGS-b-(PCL-ran-PGA) NPs can efficiently transfer siRNA targeting HIF-1 $\alpha$  into cancer cells in vivo. In accordance with the finding of tumor regression, the decrease in expression levels of HIF-1 $\alpha$  mRNA and protein and increase of cell necrosis and apoptosis were also found in the HIF-1 $\alpha$  siRNA-loaded NP treatment group. Thus, this efficient delivery vector for HIF-1 $\alpha$  siRNA may be used for NPC therapy. Further studies in our laboratory will focus on the cationic surface modification of TPGS-b-(PCL-ran-PGA) NPs and deliver siRNA in combination with anticancer drugs such as cisplatin into different NPC cell lines and animal models in order to investigate

whether combination of gene therapy and chemotherapy mediated by the NP delivery system would have enhanced antitumor effect.

## Conclusion

In this research, the TPGS-b-(PCL-ran-PGA) diblock copolymer was synthesized successfully to serve as a vector for siRNA targeting HIF-1 $\alpha$  in NPC therapy. The results revealed that the NPs could efficiently deliver siRNA into CNE-2 cells and the expression level of HIF-1 $\alpha$  was effectively inhibited. The cytotoxicity of the CNE-2 cells was significantly enhanced by siRNA targeting HIF-1 $\alpha$ -loaded NPs when compared with the results in the control groups. The in vivo study confirmed that siRNA targeting HIF-1 $\alpha$ -loaded NPs could effectively inhibit tumor growth in nude mouse models. Thus, our study suggested that TPGS-b-(PCL-ran-PGA) NPs can function as an efficient candidate for siRNA delivery. To our knowledge, this is the first report on the fabrication of siRNA targeting HIF-1 $\alpha$ -loaded TPGS-b-(PCL-ran-PGA) NPs and its application in NPC gene therapy.

## Acknowledgments

This work was supported by the Special Fund for the development of strategic emerging industries of Shenzhen, People's Republic of China (number JCYJ20120830162655505 to XM Li) and the Open Research Fund Program of the State Key Laboratory of Virology of China (number 2013006 to Y Zheng).

## Disclosure

The authors report no conflicts of interest in this work.

## References

- Chen Y, Yang L, Huang S, et al. Delivery system for DNazymes using arginine-modified hydroxyapatite nanoparticles for therapeutic application in a nasopharyngeal carcinoma model. *Int J Nanomedicine*. 2013;8:3107–3118.
- Sarmiento MPCB, Mejia MBA. Preliminary assessment of nasopharyngeal carcinoma incidence in the Philippines: a second look at published data from four centers. *Chin J Cancer*. 2014;33(3):159–164.
- Ji RC. Hypoxia and lymphangiogenesis in tumor microenvironment and metastasis. *Cancer Lett*. 2014;346(1):6–16.
- Raval RR, Lau KW, Tran MG, et al. Contrasting properties of hypoxia-inducible factor 1 (HIF-1) and HIF-2 in von Hippel-Lindau-associated renal cell carcinoma. *Mol Cell Biol*. 2005;25(13):5675–5686.
- Rankin EB, Giaccia AJ. The role of hypoxia-inducible factors in tumorigenesis. *Cell Death Differ*. 2008;15(4):678–685.
- Hu Y, Liu J, Huang H. Recent agents targeting HIF-1 $\alpha$  for cancer therapy. *J Cell Biochem*. 2013;114(3):498–509.
- Hui EP, Chan AT, Pezzella F, et al. Coexpression of hypoxia-inducible factors 1 $\alpha$  and 2 $\alpha$ , carbonic anhydrase IX, and vascular endothelial growth factor in nasopharyngeal carcinoma and relationship to survival. *Clin Cancer Res*. 2002;8(8):2595–2604.
- Wan XB, Fan XJ, Huang PY, et al. Aurora-A activation, correlated with hypoxia-inducible factor-1 $\alpha$ , promotes radiochemoresistance and predicts poor outcome for nasopharyngeal carcinoma. *Cancer Sci*. 2012;103(8):1586–1594.
- Xueguan L, Xiaoshen W, Yongsheng Z, Chaosu H, Chunying S, Yan F. Hypoxia inducible factor-1 $\alpha$  and vascular endothelial growth factor expression are associated with a poor prognosis in patients with nasopharyngeal carcinoma receiving radiotherapy with carbogen and nicotinamide. *Clin Oncol (R Coll Radiol)*. 2008;20(8):606–612.
- Tokatlian T, Segura T. siRNA applications in nanomedicine. *Wiley Interdiscip Rev Nanomed Nanobiotechnol*. 2010;2(3):305–315.
- Varkouhi AK, Verheul RJ, Schiffelers RM, Lammers T, Storm G, Hennink WE. Gene silencing activity of siRNA polyplexes based on thiolated N,N,N-trimethylated chitosan. *Bioconjug Chem*. 2010;21(12):2339–2346.
- Ofek P, Fischer W, Calderon M, Haag R, Satchi-Fainaro R. In vivo delivery of small interfering RNA to tumors and their vasculature by novel dendritic nanocarriers. *FASEB J*. 2010;24(9):3122–3134.
- Su W-P, Cheng F-Y, Shieh D-B, Yeh C-S, Su W-C. PLGA nanoparticles codeliver paclitaxel and Stat3 siRNA to overcome cellular resistance in lung cancer cells. *Int J Nanomedicine*. 2012;7:4269–4283.
- Tamura A, Nagasaki Y. Smart siRNA delivery systems based on polymeric nanoassemblies and nanoparticles. *Nanomedicine*. 2010;5(7):1089–1102.
- Zhou J, Wu J, Hafdi N, Behr J-P, Erbacher P, Peng L. PAMAM dendrimers for efficient siRNA delivery and potent gene silencing. *Chem Commun*. 2006;22:2362–2364.
- Geusens B, Lambert J, De Smedt SC, Buyens K, Sanders NN, Van Gele M. Ultra-deformable cationic liposomes for delivery of small interfering RNA (siRNA) into human primary melanocytes. *J Control Release*. 2009;133(3):214–220.
- Park TG, Jeong JH, Kim SW. Current status of polymeric gene delivery systems. *Adv Drug Deliv Rev*. 2006;58(4):467–486.
- Son S, Kim WJ. Biodegradable nanoparticles modified by branched polyethylenimine for plasmid DNA delivery. *Biomaterials*. 2010;31(1):133–143.
- Blum JS, Saltzman WM. High loading efficiency and tunable release of plasmid DNA encapsulated in submicron particles fabricated from PLGA conjugated with poly-L-lysine. *J Control Release*. 2008;129(1):66–72.
- Davis ME, Zuckerman JE, Choi CH, et al. Evidence of RNAi in humans from systemically administered siRNA via targeted nanoparticles. *Nature*. 2010;464(7291):U1067–U1140.
- Petros RA, DeSimone JM. Strategies in the design of nanoparticles for therapeutic applications. *Nat Rev Drug Discov*. 2010;9(8):615–627.
- Woodrow KA, Cu Y, Booth CJ, Saucier-Sawyer JK, Wood MJ, Saltzman WM. Intravaginal gene silencing using biodegradable polymer nanoparticles densely loaded with small-interfering RNA. *Nat Mater*. 2009;8(6):526–533.
- Huang L, Chen H, Zheng Y, et al. Nanoformulation of D-alpha-tocopheryl polyethylene glycol 1000 succinate-b-poly(epsilon-caprolactone-ran-glycolide) diblock copolymer for breast cancer therapy. *Integr Biol*. 2011;3(10):993–1002.
- Ma Y, Zheng Y, Liu K, et al. Nanoparticles of poly(lactide-co-glycolide)-d-alpha-tocopheryl polyethylene glycol 1000 succinate random copolymer for cancer treatment. *Nanoscale Res Lett*. 2010;5(7):1161–1169.
- Collnot EM, Baldes C, Wempe MF, et al. Mechanism of inhibition of P-glycoprotein mediated efflux by vitamin E TPGS: Influence on ATPase activity and membrane fluidity. *Mol Pharm*. 2007;4(3):465–474.
- Zhang Z, Mei L, Feng S-S. Vitamin E D-alpha-tocopheryl polyethylene glycol 1000 succinate-based nanomedicine. *Nanomedicine*. 2012;7(11):1645–1647.
- Constantinou C, Papas A, Constantinou AI. Vitamin E and cancer: An insight into the anticancer activities of vitamin E isomers and analogs. *Int J Cancer*. 2008;123(4):739–752.



28. Neuzil J, Tomasetti M, Zhao Y, et al. Vitamin E analogs, a novel group of “mitocans,” as anticancer agents: The importance of being redox-silent. *Mol Pharmacol*. 2007;71(5):1185–1199.
29. Youk HJ, Lee E, Choi MK, et al. Enhanced anticancer efficacy of alpha-tocopheryl succinate by conjugation with polyethylene glycol. *J Control Release*. 2005;107(1):43–52.
30. Qiu B, Ji M, Song X, et al. Co-delivery of docetaxel and endostatin by a biodegradable nanoparticle for the synergistic treatment of cervical cancer. *Nanoscale Res Lett*. 2012;7:666.
31. Zheng Y, Chen H, Zeng X, et al. Surface modification of TPGS-b-(PCL-ran-PGA) nanoparticles with polyethyleneimine as a co-delivery system of TRAIL and endostatin for cervical cancer gene therapy. *Nanoscale Res Lett*. 2013;8:161.
32. Kung AL, Wang S, Klco JM, Kaelin WG, Livingston DM. Suppression of tumor growth through disruption of hypoxia-inducible transcription. *Nat Med*. 2000;6(12):1335–1340.
33. Stoeltzing O, McCarty MF, Wey JS, et al. Role of hypoxia-inducible factor 1 alpha in gastric cancer cell growth, angiogenesis, and vessel maturation. *J Natl Cancer Inst*. 2004;96(12):946–956.
34. Zhang X, Kon T, Wang H, et al. Enhancement of hypoxia-induced tumor cell death in vitro and radiation therapy in vivo by use of small interfering RNA targeted to hypoxia-inducible factor-1 alpha. *Cancer Res*. 2004;64(22):8139–8142.
35. Bartholomeusz G, Cherukuri P, Kingston J, et al. In vivo therapeutic silencing of hypoxia-inducible factor 1 alpha (HIF-1 alpha) using single-walled carbon nanotubes noncovalently coated with siRNA. *Nano Res*. 2009;2(4):279–291.
36. Fattal E, Bochota A. State of the art and perspectives for the delivery of antisense oligonucleotides and siRNA by polymeric nanocarriers. *Int J Pharm*. 2008;364(2):237–248.
37. Cun D, Jensen DK, Maltesen MJ, et al. High loading efficiency and sustained release of siRNA encapsulated in PLGA nanoparticles: Quality by design optimization and characterization. *Eur J Pharm Biopharm*. 2011;77(1):26–35.
38. Tahara K, Sakai T, Yamamoto H, Takeuchi H, Kawashima Y. Establishing chitosan coated PLGA nanosphere platform loaded with wide variety of nucleic acid by complexation with cationic compound for gene delivery. *Int J Pharm*. 2008;354(1–2):210–216.
39. Zhao S, Tan S, Guo Y, et al. pH-Sensitive docetaxel-loaded D-alpha-tocopheryl polyethylene glycol succinate-poly(beta-amino ester) copolymer nanoparticles for overcoming multidrug resistance. *Biomacromolecules*. 2013;14(8):2636–2646.
40. Gerber HP, McMurtrey A, Kowalski J, et al. Vascular endothelial growth factor regulates endothelial cell survival through the phosphatidylinositol 3'-kinase Akt signal transduction pathway – requirement for Flk-1/KDR activation. *J Biol Chem*. 1998;273(46):30336–30343.
41. Erler JT, Cawthorne CJ, Williams KJ, et al. Hypoxia-mediated down-regulation of bcl-2 and bax in tumors occurs via hypoxia-inducible factor 1-dependent and -independent mechanisms and contributes to drug resistance. *Mol Cell Biol*. 2004;24(7):2875–2889.
42. Unruh A, Ressel A, Mohamed HG, et al. The hypoxia-inducible factor-1 alpha is a negative factor for tumor therapy. *Oncogene*. 2003;22(21):3213–3220.
43. Akakura N, Kobayashi M, Horiuchi I, et al. Constitutive expression of hypoxia-inducible factor-1 alpha renders pancreatic cancer cells resistant to apoptosis induced by hypoxia and nutrient deprivation. *Cancer Res*. 2001;61(17):6548–6554.

## International Journal of Nanomedicine

### Publish your work in this journal

The International Journal of Nanomedicine is an international, peer-reviewed journal focusing on the application of nanotechnology in diagnostics, therapeutics, and drug delivery systems throughout the biomedical field. This journal is indexed on PubMed Central, MedLine, CAS, SciSearch®, Current Contents®/Clinical Medicine,

Submit your manuscript here: <http://www.dovepress.com/international-journal-of-nanomedicine-journal>

Dovepress

Journal Citation Reports/Science Edition, EMBASE, Scopus and the Elsevier Bibliographic databases. The manuscript management system is completely online and includes a very quick and fair peer-review system, which is all easy to use. Visit <http://www.dovepress.com/testimonials.php> to read real quotes from published authors.